

K₆Tl₂Sb₃, A Zintl Phase with a Novel Heteroatomic ∞ [Tl₄Sb₆¹²⁻] Chain¹

Lisheng Chi and John D. Corbett*

Ames Laboratory-DOE and Department of Chemistry, Iowa State University, Ames, Iowa 50011

Received December 18, 2000

The title compound with heteroatomic anionic chains ∞ [Tl₄Sb₆¹²⁻] has been discovered in the K–Tl–Sb system. The phase is obtained from a range of compositions near K₃TlSb_{1.5} following reaction first at 750–850 °C and then at 550 °C for one week or more. It crystallizes in the monoclinic system in space group C2/c, Z = 8, a = 9.951(1) Å, b = 17.137(3) Å, c = 19.640(6) Å, and β = 104.26(3)°. Swing-like (Tl₄Sb₆)¹²⁻ units consisting of alternating Sb and Tl atoms in four- and eight-membered rings are linked through Tl–Tl bonds to form infinite one-dimensional chains along \vec{a} . EHTB calculations and resistivity measurements show that the compound is a semiconductor.

Introduction

In the past decade, a variety of ternary compounds with heteroatomic anions from I–III–V (1–13–15) main-group systems have been discovered and characterized. These are often built of variously condensed tetrahedral [TrPn₄], trigonal [TrPn₃], or both structural units to generate versatile structural motifs (Tr = Al, Ga, In, Tl; Pn = P, As, Sb, Bi).² Among these structures, the nature of the anionic framework is collectively related to number, size, and charge of the cations and, in turn, to the atom proportions in the III–V anion and its valence electron count. Thus, the less reduced general anionic compositions [TrPn₂]³⁻ exhibit one-, two-, or three-dimensional anionic frameworks, depending on the counterations. For example, the sodium–indide–pnictide phases contain three-dimensional ∞ [InPn₂³⁻] units (Pn = P, As, Sb) with shared corners and edges, such that the pnictogen atoms about tetrahedral indium are all two-bonded.³ With fewer cations, the anionic framework of Ca₃[AlAs₂]₂⁴ is two-dimensional, and in Sr₃[InP₂]₂,⁵ the dimensionality of the anionic framework is further reduced to one in a construction related to that reported here.

Common anionic families include the (TrPn₂)²⁻, TrPn₃^{6-,6-8} Tr₂Pn₃^{3-,9,10} and Tr₃Pr₄³⁻¹¹ stoichiometries. However, examples that include Tr–Tr bonds are rare and include only Na₂Ga₃Sb₃¹² and Cs₇In₄Bi₆.¹³ The last is evidently also the sole bismuth-

containing example, whereas no thallium members of any type have been reported. This circumstance may have to do with the particular difficulties in handling compounds containing Tl and Bi in negative oxidation states without adventitious oxidation, or it may mean that stable examples containing these two are simply rare. We report here the first example of a I–Tl–V (or active metal–thallium–pnictide) compound, one that also exhibits Tl–Tl bonding. Our explorations suggest that alkali metal–Tl–Pn ternary compounds are very limited in number. Even quaternary examples with thallium seem to be limited to A₅TaTl₂As₄ for A = K, Rb.¹⁴

Experimental Section

Synthesis. The general synthesis techniques were as previously described.^{15–17} The metals were all obtained from Alfa-Aesar: K, 99.95%; Tl, 5–9s; Sb, 6–9s in metal contents. Because the reactants and products are sensitive to air and moisture, these were handled in N₂-filled gloveboxes in which moisture levels were below 0.1 ppm (vol). Before being weighed, the surfaces of K and Tl metals were cleaned with a scalpel. An exploratory synthesis proceeded with a ~200-mg mixture of K, Tl, and Sb in molar proportions of 3:1:2 that was welded inside a tantalum tube and then jacketed in a silica tube sealed under high vacuum (~10⁻⁵ Torr). The mixture was heated to 750 °C in a tubular furnace for 24 h, cooled to 550 °C at 10 °C/h, equilibrated at this temperature for 2 weeks, and then cooled to room temperature at 10 °C/h. The product consists of many well-shaped, black crystals, several of which were selected for single-crystal diffraction studies. An accurate compound composition was established by single-crystal X-ray diffraction analysis. A later reaction to gain the stoichiometric product was run at 850 °C for 10 h, cooled to 550 °C at 50 °C/h, and then equilibrated at this temperature for 1 month. The result was single-phase (≥95%) according to the Guinier powder pattern. NIST silicon was always added to the powder pattern samples as an internal standard, so as to gain more accurate lattice dimensions. Ten parallel reactions that explored composition space in the K–Tl–Sb system over a range from about 7:1:3 to 1.5:7:3 revealed no other ternary compounds. The same was true with As instead of Sb. There is an unknown new compound in Na–Tl–Sb, however.

- (1) This research was supported by the Office of the Basic Energy Sciences, Materials Sciences Division, U.S. Department of Energy. Ames Laboratory is operated for DOE by Iowa State University under Contract WB7405-Eng-82.
- (2) Eisenmann, B.; Cordier, G. In *Chemistry, Structure and Bonding of Zintl Phases and Ions*; Kauzlarich, S. M., Ed.; VCH Publishers: New York, 1996; Chapter 3.
- (3) (a) Cordier, G.; Ochmann, H. *Z. Kristallogr.* **1991**, *195*, 119; 107. (b) Blasé, W.; Cordier, G.; Somer, M. *Z. Kristallogr.* **1991**, *195*, 119.
- (4) Cordier, G.; Czech, E.; Jakowski, M.; Schäfer, H. *Rev. Chim. Miner.* **1981**, *18*, 9.
- (5) Cordier, G.; Schäfer, H.; Stelter, M. *Z. Naturforsch.* **1986**, *41B*, 1416.
- (6) Blasé, W.; Cordier, G.; Peters, K.; Somer, M.; von Schnering, H. G. *Angew. Chem., Int. Ed. Engl.* **1991**, *30*, 326.
- (7) von Schnering, H. G.; Somer, M.; Walz, L.; Peters, K.; Cordier, G.; Blasé, W. *Z. Kristallogr.* **1990**, *193*, 299.
- (8) Somer, M.; Walz, L.; Peters, K. *Z. Kristallogr.* **1990**, *193*, 301.
- (9) Cordier, G.; Ochmann, H. *Z. Kristallogr.* **1991**, *195*, 295.
- (10) Cordier, G.; Ochmann, H.; Schäfer, H. *Rev. Chim. Miner.* **1985**, *22*, 58.
- (11) Birdwhistell, T. L. T.; Stevens, E. D.; O'Connor, C. J. *Inorg. Chem.* **1990**, *29*, 3892.

- (12) Cordier, G.; Ochmann, H.; Schäfer, H. *Mater. Res. Bull.* **1986**, *21*, 331.
- (13) Bobev, S.; Sevov, S. *Inorg. Chem.* **1999**, *38*, 2672.
- (14) Huang, D.-P.; Corbett, J. D. *Inorg. Chem.* **1998**, *37*, 4006.
- (15) Dong, Z.-C.; Corbett, J. D. *J. Am. Chem. Soc.* **1994**, *116*, 3429.
- (16) Dong, Z.-C.; Corbett, J. D. *J. Am. Chem. Soc.* **1995**, *117*, 6447.
- (17) Dong, Z.-C.; Corbett, J. D. *Angew. Chem., Int. Ed. Engl.* **1996**, *35*, 1006.

Table 1. Selected Crystal Data and Refinement Parameters for $K_6Tl_2Sb_3$

fw	1008.59
space group, Z	$C2/c$ (No. 15), 8
lattice param ^a (Å, deg, Å ³)	
a	9.951(1)
b	17.137(3)
c	19.640(6)
β	104.26(3)
V	3245.8(9)
ρ_{calc} , Mg/m ³	4.140
μ (Mo $K\alpha$), cm ⁻¹	262.9
residuals; $R1$, $wR2$ ^b	0.0415; 0.100

^a Refined from Guinier data with Si as an internal standard, $\lambda = 1.540562$ Å, 23 °C. ^b $R1 = \sum ||F_o| - |F_c|| / \sum |F_o|$; $wR2 = [\sum w(|F_o|^2 - |F_c|^2)^2 / \sum w(F_o^2)]^{1/2}$.

Resistivity. The electrical resistivities of the phase were measured by the electrodeless "Q" method.¹⁸ A powdered 120-mg sample of the single-phase product was sieved to have a 150–250- μm range of grain sizes and diluted with chromatographic Al_2O_3 . The measurements were made at 34 MHz in the range of 100–290 K. The room-temperature resistivity obtained for $K_6Tl_2Sb_3$ is about $7.7 \times 10^2 \mu\Omega \cdot \text{cm}$. The data show a small negative temperature dependence $\partial\rho/\rho\partial T$ of $-0.3\% \text{ K}^{-1}$.

Structure Determination. Several black, well-shaped crystals of $K_6Tl_2Sb_3$ were picked up in a N_2 -filled glovebox and sealed in thin-walled capillaries. Laue and Weissenberg photographs were employed to check the singularity of crystals. A rectangular one with approximate dimensions of $0.1 \times 0.15 \times 0.45$ mm was chosen for data collection, which was carried out at room temperature on a Rigaku AFC6R diffractometer with the aid of graphite-monochromated Mo $K\alpha$ radiation. A least-squares refinement of the settings of 21 centered reflections in the range of $13^\circ < 2\theta < 15^\circ$ provided a centered monoclinic cell with dimensions of $a = 9.944(2)$ Å, $b = 17.033(3)$ Å, $c = 19.695(4)$ Å, and $\beta = 104.05(3)^\circ$. A Laue check revealed a $2/m$ crystal class. Diffraction data were collected with ω - 2θ scans up to 55° .

The TEXSAN program package¹⁹ was used for data reduction. The diffraction data were corrected empirically for Lorentz and polarization effects and for absorption with the aid of ψ -scans of three reflections ($\mu = 262.9 \text{ cm}^{-1}$). The intensity statistics ($\langle E^2 - 1 \rangle = 1.068$) and the associated systematic absences ($h + k = 2n$ for hkl ; $l = 2n$ for $h0l$) for the 3952 reflections in one hemisphere measured to $2\theta = 55^\circ$ suggested the unique centrosymmetric monoclinic space group $C2/c$. The successful refinement of the structure confirmed this assignment.

The SHELXTL²⁰ program package was used for structure solution, and this was refined by the full-matrix least-squares method on F^2 for all data. Application of direct methods revealed five heavy atom positions, two of which were assigned to Tl atoms and three to Sb atoms on the basis of both bond distances and peak heights. A subsequent difference Fourier synthesis revealed seven other independent peaks, which were all easily assigned to K atoms on consideration of the distances from these peaks to Tl and Sb. The refinement of all positions with isotropic thermal parameters proceeded smoothly to $R = 5.35\%$ with the highest residual electron density peak of $6.26 \text{ e}/\text{\AA}^3$. After a second extinction correction was applied, the final anisotropic refinement converged at $R1 = 4.15\%$, $wR2 = 10.02\%$, and $GOF = 1.029$ for 102 variables and 1758 independent observed reflections ($I > 2\sigma(I)$). The highest residual peaks in the final difference Fourier map were $3.587 \text{ e}/\text{\AA}^3$ (1.00 Å from Tl1) and $-2.037 \text{ e}/\text{\AA}^3$. The first as well as all other notable positive residues were within 1.0 Å of a Tl atom.

Some details of the crystallographic and refinement parameters are given in Table 1, the atomic positional and isotropic equivalent displacement parameters are listed in Table 2, and the important interatomic distances in the anion are given in Table 3. More detailed

Table 2. Atomic Coordinates (10^4) and Equivalent Isotropic Displacement Parameters ($\text{\AA}^2 \times 10^3$) for $K_6Tl_2Sb_3$

	x	y	z	U_{eq}^a
Tl1	6453(1)	856(1)	7278(1)	26(1)
Tl2	7897(1)	850(1)	5707(1)	26(1)
Sb1	6582(2)	2280(1)	6358(1)	22(1)
Sb2	8775(1)	890(1)	8684(1)	22(1)
Sb3	6668(2)	-603(1)	6388(1)	23(1)
K1	0	238(4)	2500	30(2)
K2	0	7995(4)	2500	31(2)
K3	314(5)	934(3)	4461(2)	38(1)
K4	3281(5)	-844(3)	6768(2)	35(1)
K5	3327(5)	2558(3)	6777(2)	31(1)
K6	9439(5)	2729(3)	5533(2)	32(1)
K7	4095(5)	746(3)	5541(2)	33(1)

^a U_{eq} is defined as one-third of the trace of the orthogonalized U_{ij} tensor.

Table 3. Nearest-Neighbors Distances (Å) in the $Tl_2Sb_3^{6-}$ Anion Unit

Tl1–Sb1	3.049(2)	Sb1–Tl1	3.049(2)
Tl1–Sb2	3.147(2)	Sb1–Tl2	3.179(2)
Tl1–Sb3	3.078(2)	Sb2–Tl1	3.147(2)
Tl1–Tl1	3.217(2)	Sb2–Tl2	3.236(2)
Tl2–Sb1	3.179(2)	Sb3–Tl1	3.078(2)
Tl2–Sb2	3.236(2)	Sb3–Tl2	3.195(2)
Tl2–Sb3	3.195(2)		

crystallographic and refinement data and all of the distances around the cations are contained in the Supporting Information. This as well as the F_o/F_c listings are also available from J.D.C.

EHTB Calculations. All the calculations were carried out using the CAESAR program package developed by Whangbo et al.²¹ The following atomic orbital energies and exponents therefore were employed for the calculations (H_{ii} = orbital energy, eV; ζ = Slater exponent). Tl (6s: -11.6, 2.3; 6p: -5.8, 1.6); Sb (5s: -18.8, 2.323; 5p: -11.7, 1.999). As is customary, the potassium atoms were not included in the calculation because of the lack of good orbital parameters for them.

Results and Discussion

Structure. The compound $K_6Tl_2Sb_3$ contains the first example of a Tl–Tl bond in a polyanion in a I–III–V system. It can be considered to contain formal K^+ ions with their valence electrons, in effect, completely transferred to covalently bonded anionic $^1[Tl_4Sb_6^{12-}]$ chains. The cell is shown in Figure 1. A second chain displaced by $1/2, 1/2, 0$ (that is, C-centered) is shown behind the darker one. The heteratomic repeat unit $[Tl_4Sb_6]^{12-}$ is displayed in Figure 2. Four-membered Tl1–Sb1–Tl2–Sb3 rings that are slightly folded at Sb1–Sb3 are interlinked by two Sb2-bridging atoms to generate the swing-like repeat unit, and these are interlinked by trans Tl1–Tl1 bonds into infinite one-dimensional $^1[Tl_4Sb_6^{12-}]$ chains. All the constituent elements of the anion are in general positions, and the chains contain only 2-fold symmetry elements that are normal to the centers of both the large rings (0, $y, 1/4$, etc., Figure 1) and the Tl1–Tl1 bonds. All Sb atoms are 2-bonded, Tl1 is 4-bonded, and Tl2 is 3-bonded. The cations reside between the chains and are in general positions except that K1 and K2 lie along the 2-fold axes. Each antimony has seven or eight near-neighbor cations, Tl1 has five, and Tl2 has six.

The Tl1–Tl1 bond would be expected to be a normal 2-electron–2-center bond (below), and at 3.217(2) Å, it is quite close to the 3.236 Å value for the diamond sublattice of Tl in

(18) Zhao, J.-T.; Corbett, J. D. *Inorg. Chem.* **1995**, *34*, 378.

(19) TEXSAN for Windows: *Crystal Structure Analysis Package*; Molecular Structure Corporation: The Woodlands, TX, 1997.

(20) SHELXTL; Bruker AXS, Inc.: Madison, WI, 1997.

(21) Ren, J.; Liang, W.; Whangbo, M.-H. *CAESAR for Windows*; Prime-Color Software, Inc., North Carolina State University: Raleigh, NC, 1998.

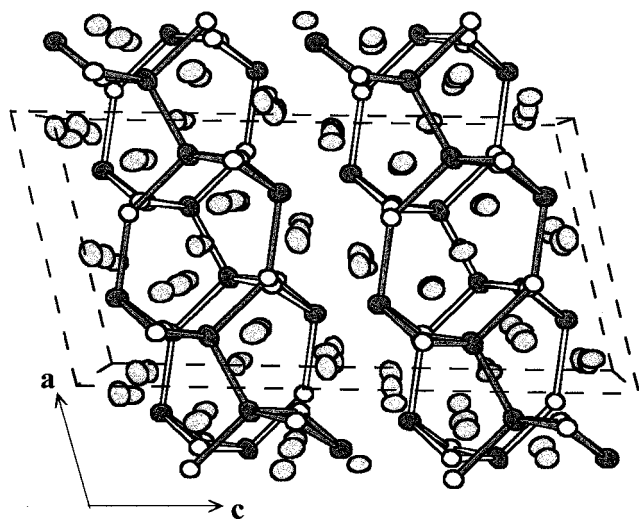


Figure 1. Perspective $\sim[010]$ view of the structure of monoclinic $K_6Ti_2Sb_3$ with its $^{12-}[Ti_4Sb_6]$ anionic chains (70% probability thermal ellipsoids). Thallium is represented by black, antimony is represented by white, and potassium is represented by gray-shaded ellipsoids. The overlapping chains are related by C-centering ($1/2, 1/2, 0$) with darker bonds in the closer chain.

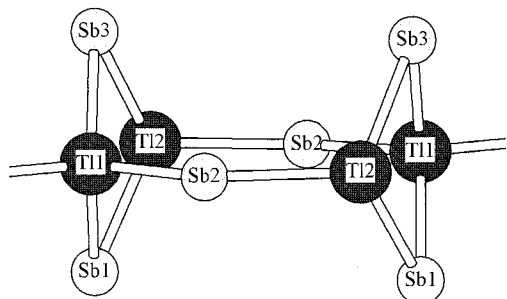


Figure 2. Side view of the $[Ti_4Sb_6]^{12-}$ repeat unit in $K_6Ti_2Sb_3$ with 2-bonded Sb, 3-bonded Ti2, and 4-bonded Ti1.

$NaTi$.^{22,23} It also lies within the fairly wide range of Ti–Ti distances, about 3.15–3.40 Å, found in a diverse collection of electron-deficient clusters with delocalized bonding,²⁴ although some as short as 3.07 Å have been found in networks.²⁵ There thus seems to be no bond lengthening from nonbonding pair repulsions across the bond. The Ti1–Ti2 separation, 3.714(1) Å, is well outside of a reasonable bonding distance. The average bond distances for Ti1–Sb and Ti2–Sb are 3.091 and 3.203 Å, respectively. That for the former set, which pertain to 4-bonded Ti1, is in good agreement with the sum of covalent radii, 3.04 Å, derived from the Ti–Ti distance in NaTi and the separation between 2-bonded Sb in KSb_2 , 2.842(2) Å.²⁶ Any effect of nonbonding pair repulsion between atoms bonded to Ti1 would again seem to be marginal. On the other hand, the average Ti2–Sb distance about the 3-bonded atom that is formally Ti^{2-} is 0.11 Å larger. The angles around Ti1 and Ti2 average 109.5° and 106.0°, respectively, also appropriate to the expectation that the more-reduced Ti2 is more or less surrounded by three Sb atoms and a lone pair.

The structural unit $[Ti_4Sb_6]^{12-}$ is similar to those in $Ca_3-[GaAs_2]_2$ and $Ca_3[InAs_2]_2$,^{4,5} but the condensation modes are

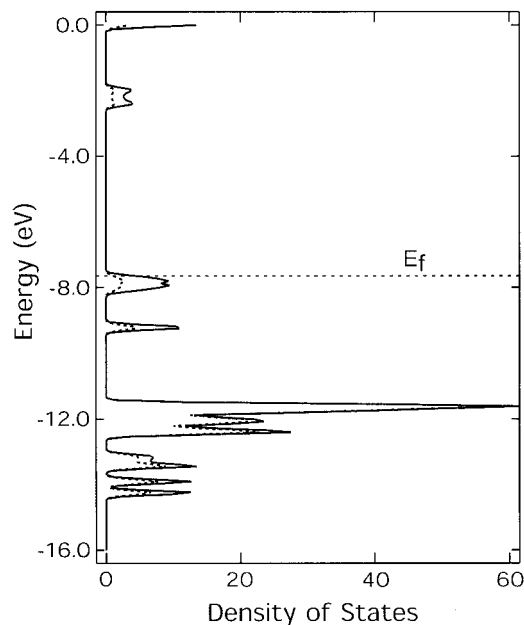


Figure 3. Total DOS (solid) and the projection of the total antimony components (dashed) calculated for the infinite $^{12-}[Ti_4Sb_6]$ chains in $K_6Ti_2Sb_3$.

quite different. The anionic structure of the former contains comparable $[Ga_4As_6]$ units, but these are connected to four others by arsenic bridges to produce a $(Ga_4As_6)_{As_{4/2}} = GaAs_2$ stoichiometry in a two-dimensional framework. In the indium analogue, similar units are linked through shared pairs of indium atoms into one-dimensional chains. The 2-bonded antimony atoms in the present compound have an oxidation state of -1 , and their further condensation via some neutral three-bonded Sb^0 atoms may be possible with a reduced number of cation charges and, perhaps, altered sizes.

Electronics. As seen, $K_6Ti_2Sb_3$ contains three nonequivalent Sb atoms and two nonequivalent Ti atoms. If, as is customary, a complete transfer of the valence electrons from potassium to the post-transition elements is assumed for the purpose of oxidation-state counting, the anion is seen to attain octet states for all atoms and with only 2-electron–2-center bonding. Thus, the Ti1, Ti2, and Sb atoms possess 0, 1, and 2 lone pairs, respectively, according to the conventional scheme for a classic Zintl phase. A slightly different expression of this in a style often attributed to von Schnering²⁷ is $[(4b-Ti1^-)(3b-Ti2^{-2})(2b-Sb^-)_3] = Ti_2Sb_3^{6-}$. With only s and p valence orbitals on the atoms, the repeat unit $[Ti_4Sb_6]^{12-}$ has $(4 \times 4) + (6 \times 4) = 40$ orbitals. These occur as 13 bonds (Figure 2), $6(2) + 2 = 14$ filled nonbonding orbitals (electron pairs) and 13 empty antibonding orbitals, the first two containing 54 valence electrons. The compound is thus closed-shell and is expected to exhibit a band gap below a higher-lying potassium-based conduction band. This is in agreement with its measured $\rho_{290} \approx 770 \mu\Omega \cdot cm$ and the negative temperature coefficient of resistivity (Experimental Section).

To better understand the energetic distribution of the bonding and nonbonding pairs, an electronic band calculation was carried out on the one-dimensional $[Ti_4Sb_6]^{12-}$ chain. Figure 3 gives both the total and the projected (dashed) antimony partial densities-of-states (DOS) curves for the chain. As expected, the narrow bands suggest that the electron densities in this compound are largely localized. As judged from COOP curves

(22) Schmidt, P. C. *Struct. Bonding (Berlin)* **1987**, 65, 91.

(23) Dong, Z.-C.; Corbett, J. D. *Inorg. Chem.* **1996**, 35, 2301.

(24) Source of references to original articles: Corbett, J. D. *Angew. Chem., Int. Ed.* **2000**, 39, 670.

(25) Dong, Z.-C.; Corbett, J. D. *Inorg. Chem.* **1996**, 35, 1444.

(26) Rehr, A.; Guerra, F.; Barkin, S.; Hope, H.; Kauzlarich, S. M. *Inorg. Chem.* **1995**, 34, 6218.

(27) von Schnering, H.-G. *Angew. Chem., Int. Ed. Engl.* **1981**, 20, 33.

(not shown), bands below -19 eV (out of the energy window) are largely derived from Sb 5s and some Tl 6s. Of the six clear bands between -14.4 and -11.5 eV, the lowest three all reflect Tl(s)–Sb bonding, with somewhat more Tl1 contributions in the bottommost one. The fourth and fifth are mainly Tl(p)–Sb, while the largest band at -11.7 eV ($= H_{ii}$ for Sb p) is principally Sb lone pairs.

The band at -9.2 eV represents the Tl1–Tl1 bond but with an appreciable antibonding Tl1–Sb component according to the COOP data. In parallel, the peak just below E_F originates with only antibonding Tl2–Sb interactions, presumably between the lone pairs on each. The longer Tl2–Sb bonds have appropriately lower overlap populations, about 25% less than for the same

number of shorter Tl1–Sb bonds. It should be noted that Figure 3 does not show a plausible band gap because the cations, which should make substantial contributions to the conduction band, were not included in the calculation.

Acknowledgment. We thank D.-K. Seo for helpful discussions.

Supporting Information Available: Tables of additional crystallographic and refinement parameters and a complete listing of nearest-neighbor distances. This material is available free of charge via the Internet at <http://pubs.acs.org>.

IC0014134